electronics

MDPI

Article

Model for the Prediction of Rain Attenuation Affecting Free Space Optical Links

Umair Ahmed Korai [1,2], Lorenzo Luini [3,4,*] and Roberto Nebuloni [4]

1 Department of Electronic and Electrical Engineering, University of Strathclyde, Glasgow G1 1XW, UK; umair.korai@strath.ac.uk or umair.korai@faculty.muet.edu.pk
2 Department of Telecommunication Engineering, Mehran University of Engineering and Technology, Jamshoro 76062, Sindh, Pakistan
3 DEIB, Politecnico di Milano, Piazza Leonardo da Vinci, 32, 20133 Milan, Italy
4 IEIIT, Consiglio Nazionale delle Ricerche, Piazza Leonardo da Vinci, 32, 20133 Milan, Italy; roberto.nebuloni@ieiit.cnr.it
* Correspondence: lorenzo.luini@polimi.it; Tel.: +39-02-2399-3693

Received: 27 September 2018; Accepted: 5 December 2018; Published: 7 December 2018

Abstract: A model for the prediction of the attenuation induced by rain on free space optical (FSO) links is presented. The proposed methodology is developed, starting from the accurate simulation of the interaction between FSO links (path length up to 5 km) and precipitation maps, from which analytical expressions are then proposed. The model is simple as it only receives the local rainfall statistics for the site of interest as the input, but it is also accurate, as it takes into account the dependence of the attenuation on the drop size distribution (DSD), as well as multiple scattering effects associated with rain, which contributes to reducing the overall predicted attenuation. The proposed model represents a useful tool to dimension FSO links in areas where fog is negligible, i.e., where rain has the highest impact on the link performance.

Keywords: free space optics; rain attenuation; multiple scattering; electromagnetic wave propagation

1. Introduction

Optical wireless communications are based on the transmission of data through the atmosphere using optical carriers within spectral windows that are free from molecular absorption. Optical links target very short-range (in the order of few cm), as well as long-range (hundreds of km), applications. Specifically, the terms free space optical communications or free-space optics (FSO) typically refer to outdoor terrestrial links operating over distances from a few tens of meters up to several kilometers.

As optical wavelengths are very sensitive to atmospheric effects, FSO has been so far restricted to niche applications, such as inter-building connectivity in enterprise/campus environments, temporary links in emergency situations, or high-definition video transmission (typically from TV cameras to a broadcasting center) [1]. However, with the dramatic growth of broad-band services over wireless cellular networks for mobile users, FSO might emerge as a competitor of microwave wireless systems for backhauling in future 5G meshes, where the cell size, hence the distance between base stations, is relatively small [2].

Indeed, FSO presents several advantages over radiofrequency, including a very high-bandwidth, narrow-beam transmission (which, in turn, improves security, re-use capability, and electromagnetic compatibility issues), no licensing costs, and simple installation. On the other hand, the performance of FSO is strongly limited by atmospheric effects [3,4]. In clear air, atmospheric turbulence is the cause of signal fluctuations (scintillations) that may affect FSO operation [5]. Spatial diversity at the receiver (by aperture averaging or multiple apertures) and/or at the transmitter (by multiple transmit beams)

is a viable solution to reduce the detrimental effect of turbulence. Mitigation techniques also include adaptive transmission (where the transmit power, the modulation, and/or the coding are adjusted to the actual channel conditions), and cooperative transmission through multi-hop or parallel relaying [1]. Laser beam propagation through atmospheric particles (fog, rain, snow, etc.) may produce long and deep signal fades that result in link outage [6–8]. In this case, the techniques used for turbulence mitigation are ineffective due to the correlation scale of the process (in both time and space). Fog has the most detrimental impact on optical waves: specific attenuation due to dense fog is as high as 300 dB/km for a visibility of around 50 m [9]. Rain attenuation, although markedly dependent on the microphysics of precipitation, is of the same order of magnitude as at mm-waves. As a matter of fact, where fog occurrence is non-negligible, FSO is outperformed by microwave links in high-availability applications. On the other hand, in sites where fog is not present, such as inland tropical/equatorial regions, rain is the main atmospheric constituent limiting the length and performance of FSO links. It is therefore of key importance to properly investigate the impact of rain on FSO links.

Several global models have been developed and proposed in the literature to predict rain attenuation on terrestrial links operating at frequencies in the millimeter-/micro-wave portion of the spectrum. The International Telecommunication Union—Radio communication sector (ITU—R) P.530-16 [10], the Brazilian [11], the Lin [12], and the Moupfouma [13] models are worth being cited as sample methodologies that aim at being globally applicable. On the other hand, although several works in the literature investigate the effects of rain on FSO, they focus on limited local data (no long-term statistically meaningful rain attenuation datasets) and do not attempt to propose expressions of more general applicability. For instance, optical attenuation has been predicted according to a scattering model and a theoretical DSD [14]. Alternatively, empirical best-fit expressions between optical attenuation and rain rate have been proposed [7,15]. Though the above models work on an event-basis or on a local scale, they are not suitable for global scale application and statistical assessment, because rain microphysics is time-variant and depends on climatic and environmental factors.

In this context, this work describes the development of an analytical model to predict rain attenuation on FSO links for a path length L of up to 5 km, whose applicability goes beyond the single site. Indeed, the proposed model represents an innovative step forward towards providing a tool enabling to plan the deployment of FSO links in sites where the local precipitation features might differ considerably. Indeed, the model introduces significant elements of novelty, which are not available all together in any of the models presently available in the literature: (1) it aims at being widely applicable; (2) it takes into account the dependence on the DSD, which the specific rain attenuation strongly depends on; and (3) it embeds the multiple-scattering effects occurring at optical frequencies at high rain rates, which, as a matter of fact, decrease the attenuation induced by precipitation. The model development relies on realistic high-resolution synthetic rain maps to properly take into account the high spatial variability of precipitation and it takes advantage of the analytical formulation of the Lin's model, originally proposed in [12] to predict rain attenuation along millimeter-/micro-wave links and adapted in this work to the optical domain.

This paper is organized as follows: Section 2 describes the method proposed for the estimation of rain attenuation impairing FSO links based on synthetic rain maps. Section 3 reviews some models available in the literature to estimate rain attenuation in the millimeter-/micro-wave portion of the spectrum in order to investigate the adaptability and applicability of such methodologies to the prediction of rain attenuation on FSO links, which is compared to the results obtained in Section 2. The effect of multiple scattering is addressed in Section 4. Finally, Section 5 concludes the paper.

2. Predicting Rain Attenuation Impairing FSO Links

A key element limiting the development of rain attenuation models for FSO links is the lack of experimental data [7,16–18], especially long-term statistics, which are typically required in the system design phase to identify the power margin needed to cope with rain attenuation. Indeed, while a large set of rain attenuation data have been collected by links operating in the 10–100 GHz

frequency range and made available by the study group 3 of ITU−R for the development/test of rain attenuation models, this is not the case for optical wavelengths. In order to tackle the lack of experimental data, in this work, we rely on a methodology able to synthesize realistic rain fields on a global basis, i.e., multi exponential cell (MultiEXCELL) [19]. Afterwards, the relationship between rain rate and specific attenuation (i.e., attenuation per unit path length) is derived through fundamental scattering theory. Finally, rain attenuation impairing a link of an arbitrary length is obtained by integrating specific rain attenuation along the path. The results are presented in the form of the complementary cumulative distribution function (CCDF) of rain attenuation, which is the key element typically supporting the design of wireless communication systems.

2.1. MultiEXCELL

Presented in [19], MultiEXCELL is a global rainfall model oriented to the investigation and prediction of atmospheric electromagnetic wave propagation impairments. MultiEXCELL generates sets of synthetic rain fields, whose ensemble preserves the local rainfall statistics (the only input to the model) and reproduces the rainfall spatial correlation.

Synthetic rain fields, whose standard spatial resolution is 1 km × 1 km and whose lateral dimension can range between 200 and 300 km, result from the arrangement of multiple synthetic exponential cells according to the natural rain cells' aggregative process observed in radar-derived precipitation maps. Moreover, MultiEXCELL reproduces the statistical distribution of the fractional rainy area, in turn estimated from the rain amount accumulated in six-hour slots, M_t, extracted from the European centre for medium-range weather forecast (ECMWF) 40-year re-analysis (ERA40) database [20]. A key advantage of MultiEXCELL is that a relatively small set of synthetic rain fields (around 1000 maps) is sufficient to reliably represent the local rainfall process and, thus, to efficiently simulate the interaction between precipitation and wireless telecommunication systems. In fact, when tested against extensive experimental datasets, MultiEXCELL has proven to provide satisfactory results in different propagation-oriented applications and scenarios [21–23], including the prediction of rain attenuation on terrestrial radio links [24,25].

Given the strong impact of precipitation at optical frequencies, in this work, the standard spatial resolution of MultiEXCELL rain maps is increased from 1 km × 1 km to 250 m × 250 m, with the aim of providing a more accurate prediction of rain attenuation on short FSO links (up to a few kilometers).

2.2. Specific Attenuation

Specific attenuation due to rain is independent of the wavelength in the optical transmission windows usually adopted by commercial FSO systems, which are the classical 0.780–0.850 and 1.520–1.600 μm bands [9]. For practical purposes, the specific attenuation γ (in dB/km) is often calculated from the rain rate R (in mm/h) through simple power-law relationships, i.e.,

$$\gamma = kR^{\alpha}. \tag{1}$$

For a given rain rate, the coefficients k and α are rather sensitive to the distribution of raindrop size, namely to the DSD of precipitation, as clearly shown, for example, in [16]. Table 1 reports the best-fit k and α coefficient derived from the values of γ calculated through classical scattering theory [16], assuming that the DSD is modeled with a Gamma function [26], with the latter only being dependent on the so-called shape parameter μ and on the rain rate. Measurements show that μ can range between −3 and 8 [27].

Figure 1 shows the curves in (1), with the coefficients in Table 1 for six different values of μ. The DSD impact depends on R and it is higher at very low or very high rain rates. For instance, if R = 50 mm/h, γ ranges from less than 10 dB/km ($\mu = -3$) to more than 25 dB/km ($\mu = 7$). On the other side, microwave attenuation is not as sensitive to the DSD as optical attenuation. Finally, we point out that specific rain attenuation in the optical bands is of the same order of magnitude as in the V-band

(40–75 GHz): for instance, if R = 50 mm/h and μ = 1, γ = 19 dB/km at 50 GHz, whereas γ = 18 dB/km in the above optical windows.

Table 1. Coefficients in (1) for different values of the DSD shape parameter (μ).

Shape Parameter (μ)	k	α
−3	4.0684	0.2077
−2	2.2838	0.4050
−1	1.5921	0.5506
0	1.2924	0.6436
1	1.1394	0.7057
2	1.0505	0.7497
3	0.9938	0.7823
4	0.9551	0.8074
5	0.9273	0.8273
6	0.9065	0.8435
7	0.8905	0.8569
8	0.8779	0.8682

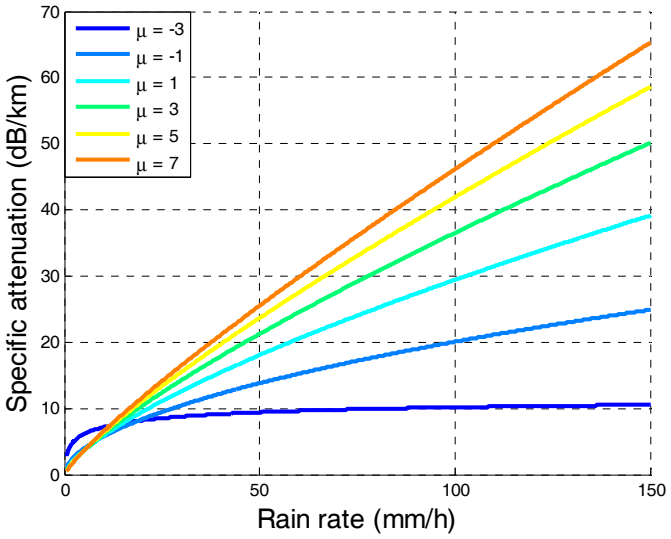

Figure 1. Specific rain attenuation (dB/km) as a function of the rain rate (mm/h) for different values of the shape parameter μ of the Gamma DSD.

2.3. Path Attenuation

The prediction of the path attenuation induced on FSO links starts from the whole set of synthetic rain fields generated by MultiEXCELL, which only requires the local CCDF of the rain rate, also known as $P(R)$ [19], as the input.

As a reference, we have considered the site of Hyderabad, Pakistan (latitude = 25.38° N, longitude = 68.37° E), which is characterized by limited precipitation through the year, besides the absence of fog. The input local $P(R)$ was estimated using the prediction model included in Annex 1 of recommendation ITU-R P.837-6 [28]. The yearly $P(R)$ curve is reported in Figure 2.

Figure 3 shows the zoom on a sample rain rate map (out of the whole set consisting of 1088 maps) generated by MultiEXCELL, whose dimension is 230 km × 230 km with a spatial resolution equal to 250 m × 250 m. For each map, the total rain attenuation A (in dB) affecting the FSO link is calculated as:

$$A = \int_L \gamma(l)dl = \int_L kR(l)^\alpha dl = \sum_{i=1}^{N} kR_i{}^\alpha \Delta l, \quad (2)$$

where L is the length of the link; k and α are the power-law coefficients in (1) and listed in Table 1; and $R(l)$ is the rain rate at position l along the path, associated with a given pixel of the rain map. The right-end term of (2) provides the discretized version of the expression to calculate the rain attenuation A, in which R_i is the rain intensity associated with the i-th pixel and Δl = 250 m. In order to increase the statistical significance of the results and to exploit the large rain maps generated by MultiEXCELL as much as possible, several attenuation values are obtained by moving the hypothetical FSO link across the synthetic rain map. As a result, each rain map is turned into an attenuation map, as shown, for example, in Figure 4 (horizontal link, L = 5 km, μ = 1).

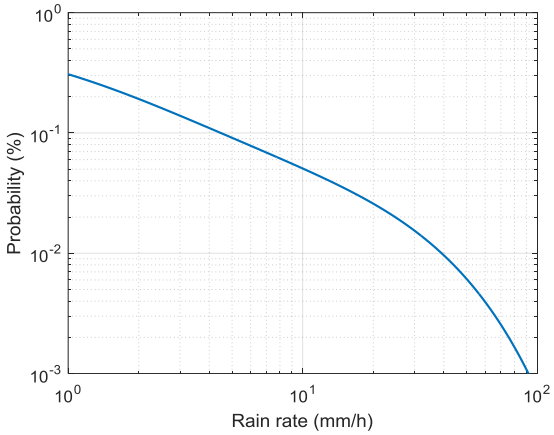

Figure 2. Yearly $P(R)$ for Hyderabad, Pakistan, estimated using recommendation ITU-R P.837-6.

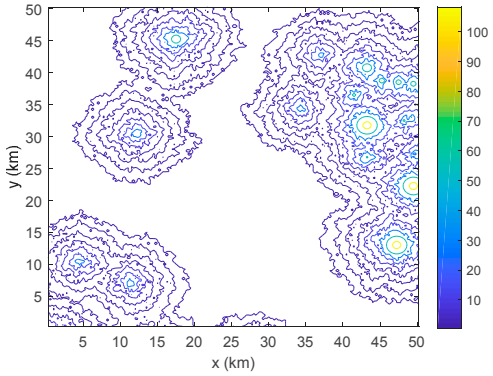

Figure 3. Zoom on a sample rain map generated for Hyderabad, Pakistan, using MultiEXCELL (colorbar indicating the rain rate in mm/h).

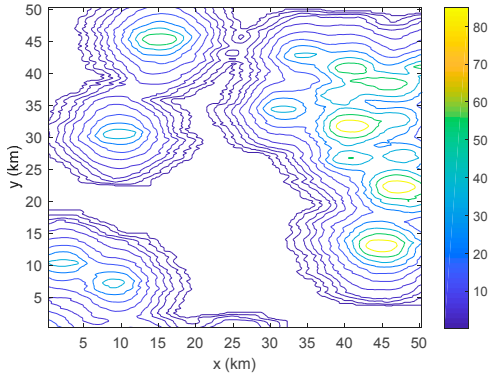

Figure 4. Zoom on a sample attenuation map (color bar indicating attenuation in dB) obtained from the rain maps in Figure 3 using (2) (5-km FSO link, power-law coefficients corresponding to μ = 1 in Table 1).

As a final step, the rain attenuation CCDF, also typically referred to as $P(A)$, is calculated by gathering all the A values associated with the set of synthetic rain maps generated by MultiEXCELL for the site of interest. Figure 5 reports the attenuation statistics for a link with L = 5 km and for different μ values. Results confirm the strong impact of the DSD on rain attenuation, as well as the high A values affecting FSO links: in the "best case", A exceeds 45 dB for the exceedance probability $P \approx 0.01\%$ of the yearly time (approximately 1 h/year).

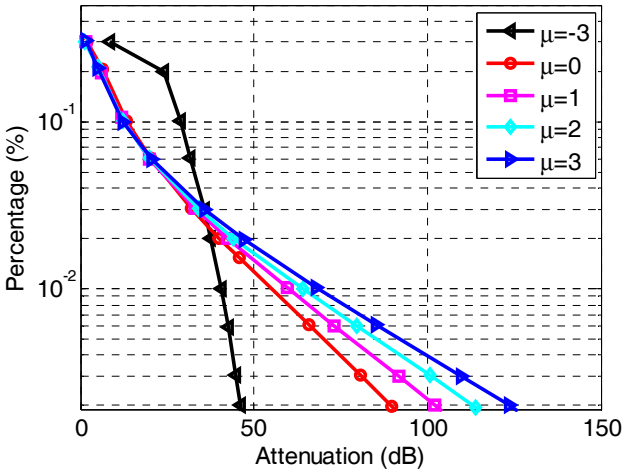

Figure 5. $P(A)$s obtained from the whole set of rain attenuation maps for Hyderabad, Pakistan (L = 5 km, different values of μ).

3. Comparison with Analytical Methods

The rain attenuation statistics estimated using the methodology described in Section 2 are expected to be accurate based on the prediction results shown in [24,25], where MultiEXCELL rain maps were used in the context of terrestrial radio links. On the other hand, the whole simulation process is rather complex and time consuming, which prompted us to search for an analytical approach aimed at predicting rain attenuation on FSO links. The rationale is to use the $P(A)$s derived from MultiEXCELL maps as the reference curves against which the prediction performance of existing analytical models can be assessed. Specifically, we have taken into account the following models, which were developed to predict rain attenuation on terrestrial radio links: ITU-R P.530-16 [10], Brazilian [11], Lin [12], and Moupfouma [13]. Indeed, all these models rely on analytical expressions that include the k and α power-law coefficients for the conversion of the rain rate into specific attenuation: the question addressed in this section is whether these models can be extended to predictions in the optical frequency range by simply using the adequate set of k and α coefficients (see Table 1). First, the models are briefly described and then their prediction performance is compared.

3.1. Rain Attenuation Models for Terrestrial Radio Links

3.1.1. ITU-R P.530-16 Model

The prediction model included in recommendation ITU-R P.530-16 [10] relies on the following steps:

1. Compute the effective path length of the link, d_{eff}, by multiplying the actual path length L (km) by the path reduction factor r, which can be expressed as:

$$r = \frac{1}{0.44L^{0.633}R_{0.01}^{0.073\alpha}f^{0.123} - 10579[1 - \exp(-0.024L)]}, \quad (3)$$

where f is the frequency in GHz; L is the path length; α is extracted from Table 1; and $R_{0.01}$ is the rain rate exceeded for 0.01% of the time in a year, to be extracted from the local $P(R)$. According to [10], if $r > 2.5$, its value is bounded to 2.5.

2. The path attenuation exceeded for 0.01% of the yearly time is calculated as:

$$A_{0.01} = \gamma_R d_{eff} = \gamma_R L r. \tag{4}$$

3. The prediction of the full $P(A)$, for $0.001\% \leq P \leq 1\%$, is given by:

$$A(P) = A_{0.01} C_1 P^{-(C_2 + C_3 \log_{10} P)}, \tag{5}$$

with C_1, C_2, and C_3 being empirical coefficients depending on frequency f [10].

3.1.2. Lin Model

Additionally, the methodology proposed by Lin in [12] takes advantage of the concept of the path reduction factor to estimate rain attenuation statistics on terrestrial links. According to this model, the rainfall attenuation exceeded for a percentage P of the yearly time can be calculated as:

$$A(P) = kR(P)^{\alpha} L r, \tag{6}$$

where L is the path length, r is the path reduction factor, k and α are the coefficients in Table 1, and $R(P)$ is the rain rate exceeded for the same percentage P of the time. The factor r takes the following simple expression:

$$r = \frac{1}{1 + L/L(R)}, \tag{7}$$

where:

$$L(R) = \frac{2623}{R(P) - 6.2}. \tag{8}$$

3.1.3. Moupfouma Model

Similarly to the ITU-R model, the prediction method proposed by Moupfouma in [13] receives $R_{0.01}$ as the input to predict A as:

$$A(P) = kR_{0.01}^{\alpha} L_{eq}(P, L). \tag{9}$$

L_{eq} in (9) is the equivalent path length that is the product between the actual path length L and a correction factor dependent on the rain rate:

$$L_{eq}(P, L) = L \exp\left(-\frac{R(P)}{1 - 100R(P)}\right). \tag{10}$$

Equation (10) is valid for $L \leq 7$ km.

3.1.4. Brazilian Model

In the model proposed by Silva Mello et al. in [11], the effective path length d_{eff} is calculated as:

$$d_{eff} = \frac{1}{1 + d/d_0} L, \tag{11}$$

where:

$$d_0 = 119R(P)^{-0.244}. \tag{12}$$

The prediction of the rain attenuation exceeded for P percent of the time is achieved as:

$$A(P) = \gamma d_{eff} = kR_{eff}^{\alpha} d_{eff}, \tag{13}$$

where R_{eff}, i.e., the effective rain rate, is:

$$R_{eff} = 1.763 R(P)^{0.753+0.197/L}. \quad (14)$$

3.2. Performance Assessment

In this section, the prediction performance of the analytical models briefly described above is evaluated. Specifically, the same $P(R)$ used to produce the set of synthetic maps through MultiEXCELL provides the input for the prediction models. As for the DSD, we have used the different values of μ listed in Table 1. Furthermore, though k and α do not depend on the wavelength λ (according to the asymptotic theory of optical scattering, which is valid for particles that are much larger than λ [29]), we have selected λ = 1.55 µm, as the ITU-R model also requires the frequency f as the input (see e.g., (3)). Finally, we have considered path lengths ranging from 1 to 5 km.

Examples of the results are shown in Figure 6, which compares the $P(A)$ as obtained numerically from MultiEXCELL maps (blue line), with the curves estimated by the models: in this case, μ = 1 and L = 1 km.

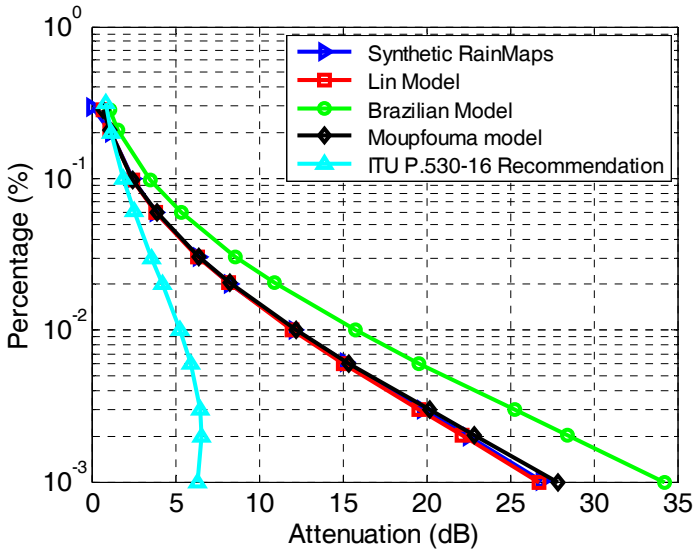

Figure 6. Assessment of the models' prediction performance: L = 1 km and μ = 1.

Both the Lin and Moupfouma models provide accurate predictions of the $P(A)$, while the worst performance is achieved by the current ITU-R method. This finding is likely due to the high number of coefficients defining the path reduction factor r in (3), which were regressed using a large set of rain attenuation statistics derived from millimeter-/micro-wave links as the reference. Furthermore, the Brazilian model has a poor performance, likely for the same reason. Similar conclusions can be drawn from Figure 7, which reports the same curves, but for a link with L = 3 km: while the Moupfouma model deviates more from the reference curve, the prediction obtained from the Lin model is still very accurate.

The models' prediction error is quantified in terms of root mean square (RMS) and mean (M) values of the following error figure ε, defined in recommendation ITU-R P.311-15 [30]:

$$\varepsilon(P) = \begin{cases} 100\left[\frac{A_m(P)}{10}\right]^{0.2} \ln\left[\frac{A_e(P)}{A_m(P)}\right] & A_m(P) \leq 10\,\text{dB} \\ 100\ \ln\left[\frac{A_e(P)}{A_m(P)}\right] & A_m(P) > 10\,\text{dB} \end{cases}, \quad (15)$$

where $A_m(P)$ and $A_e(P)$ represent the path attenuations, both corresponding to exceedance percentage P, extracted from the reference and the estimated $P(A)$, respectively.

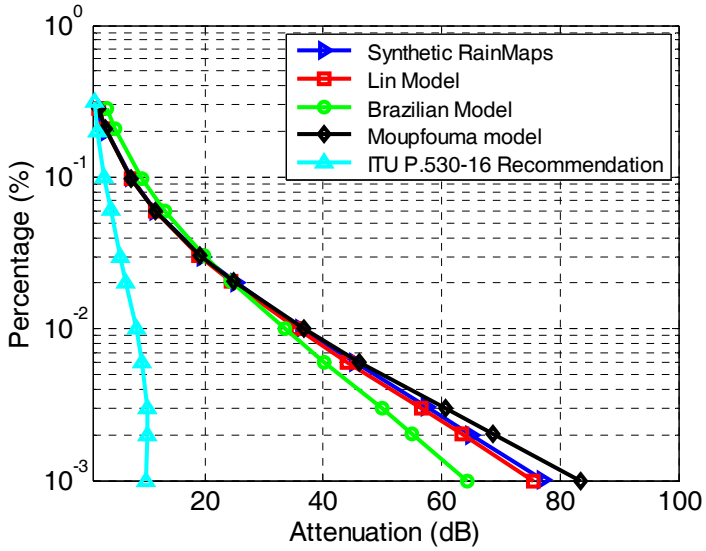

Figure 7. Assessment of the models' prediction performance: L = 3 km and μ = 1.

Figure 8 shows the mean value M (left side) and RMS (right side) of ε obtained by testing all the models considered above for various path lengths. As is clear from the figure, overall, the Lin model gives the best result (the RMS of error figure is approximately 2%), which is almost independent of L. Though not shown here for brevity's sake, very similar results were obtained for different values of μ, which allows the conclusion that the Lin model can be accurately and efficiently used to predict rain attenuation statistics on FSO links.

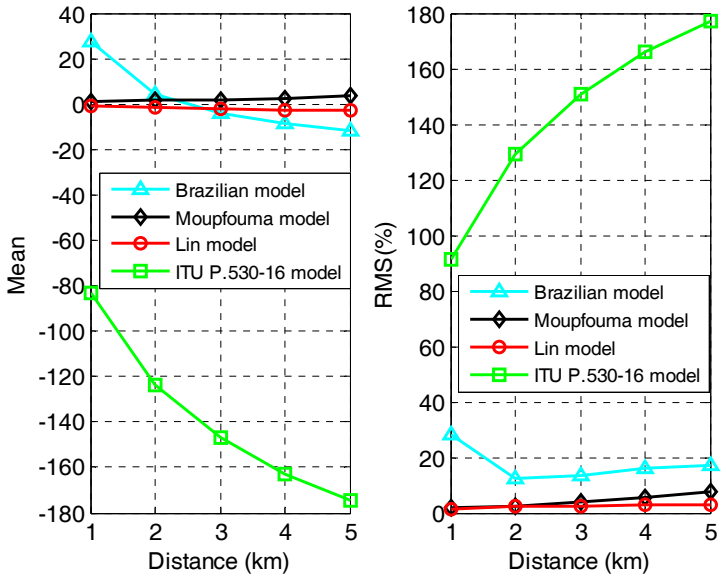

Figure 8. Mean and RMS value (left and right panel, respectively) of the error figure for different path lengths using all models for μ = 1.

4. Multiple Scattering Effects

The simple scattering theory used to derive the coefficients in (1) assumes that the electromagnetic energy associated with the portion of the wave front intercepted by a particle is lost. However, as a matter of fact, the incident energy is scattered by the particle with an angular pattern that, in the case of raindrops and optical wavelengths, exhibits a narrow peak in the forward direction. As a result, a relevant fraction of the radiation transmitted through a rainy atmospheric layer is received because of particle scattering. If the light beam undergoes several particle interactions before reaching the receiver,

the process is called multiple scattering. Forward and multiple scattering reduce path attenuation especially at high rain rates, which needs to be taken into account when devising a model to predict rain attenuation statistics for FSO links. The corresponding multiple scattering gain, which depends on the path length, is calculated here through a Monte Carlo photon propagation simulator [31].

4.1. Multiple Scattering Gain

The multiple scattering gain is defined as the ratio between the multiple scattering transmissivity and the Beer-Lambert transmissivity expressed on a dB scale, i.e.,

$$G_{ms} = 10 \log_{10}\left(\frac{\tau_{ms}}{\tau_{BL}}\right), \tag{16}$$

where

$$\tau_{BL} = e^{-\gamma L}. \tag{17}$$

In the following, G_{ms} is calculated as a function of the path length L and fitted with a power-law expression, that is,

$$G_{ms} = aL^b. \tag{18}$$

The coefficients a and b depend on the rain rate for a given DSD shape. Therefore, by taking into account the multiple scattering gain, the adjusted path attenuation can be written as follows:

$$A_{ms}(L, R) = A(L, R) - G_{ms}(L, R), \tag{19}$$

where A is the attenuation calculated through the model described in Section 2 or through one of the analytical methods listed in Section 3.

4.2. Monte-Carlo Simulation Results

In principle, the multiple-scattering gain depends not only on path length and on rain properties (primarily rain rate and DSD shape), but also on the transmitter and receiver characteristics, and on the beam type. For the sake of simplicity, the following parameters were fixed for all simulations:

- Beam type: collimated (i.e., zero divergence), transmitted beam width = 2.5 cm
- Receiver aperture: 10 cm radius (circular)
- Receiver field of view: 90° (open detector)

On the other side, different path lengths, rain rates, and DSDs were considered. As an example, the multiple scattering gain for propagation through a homogeneous rain layer is shown in Figure 9 as a function of the path length in the case $\mu = 1$. The solid lines are power-law best fits of the simulation results for seven different rain rates. Finally, Table 2 reports the values of the power-law best fit coefficients for $\mu = 1$, 2, and 3, and the above seven rain rates.

Table 2. Coefficients of the power-law relationship in (18) as a function of rain rate and DSD shape.

Rain Rate (mm/h)	$\mu = 1$		$\mu = 2$		$\mu = 3$	
	a	***b***	***a***	***b***	***a***	***b***
1	0.011	0.484	0.010	0.522	0.008	0.553
2	0.016	0.521	0.015	0.547	0.013	0.576
5	0.026	0.562	0.024	0.592	0.021	0.622
10	0.036	0.601	0.033	0.636	0.031	0.657
20	0.046	0.651	0.044	0.685	0.042	0.709
50	0.063	0.723	0.062	0.757	0.062	0.773
100	0.080	0.777	0.082	0.804	0.086	0.817

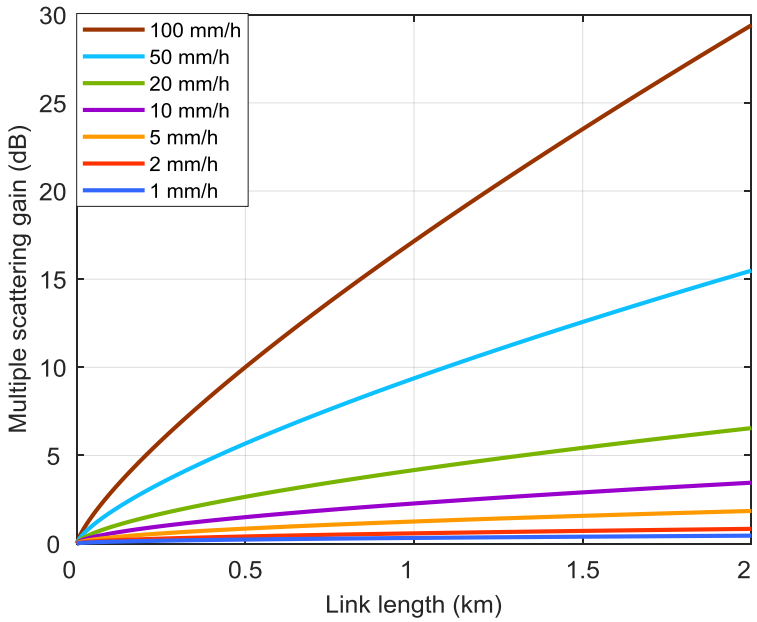

Figure 9. Multiple scattering gain (see (18)) as a function of the path length L, for optical propagation through rain. DSD: Gamma type, $\mu = 1$.

The multiple-scattering gain best-fit coefficients a and b are dependent on the rain rate R. The following polynomial best-fit is a good approximation of the measured coefficients (see Table 3):

$$a = p_0 + p_1 \ln(R) + p_2 [\ln(R)]^2, \tag{20}$$

$$b = p_0 + p_1 \ln(R) + p_2 [\ln(R)]^2. \tag{21}$$

Table 3. Polynomial best fit coefficients for a(R) and $b(R)$ in (20) and (21), respectively.

	$\mu = 1$		$\mu = 2$		$\mu = 3$	
	a	***b***	***a***	***b***	***a***	***b***
p_0	0.0112	0.4965	0.0103	0.5194	0.0092	0.5504
p_1	0.0060	0.0390	0.0040	0.0389	0.0019	0.0372
p_2	0.0019	0.0053	0.0025	0.0052	0.0031	0.0047

The difference between the multiple-scattering gain obtained from the simulations and the best-fit calculated through (18), (20), and (21) is within 15% (on a dB scale), except for the case $R = 1$ mm/h, where rain attenuation has a negligible impact on the link performance. The $P(A)$ curve including multiple-scattering for Hyderabad and the one previously shown in Figure 6 are compared in Figure 10 ($L = 1$ km and $\mu = 1$). Multiple-scattering effects produce a reduction of path attenuation in the order of 50% (on a dB scale) when a laser beam propagates through heavy rain. Similar conclusions were achieved in [14] from propagation measurements.

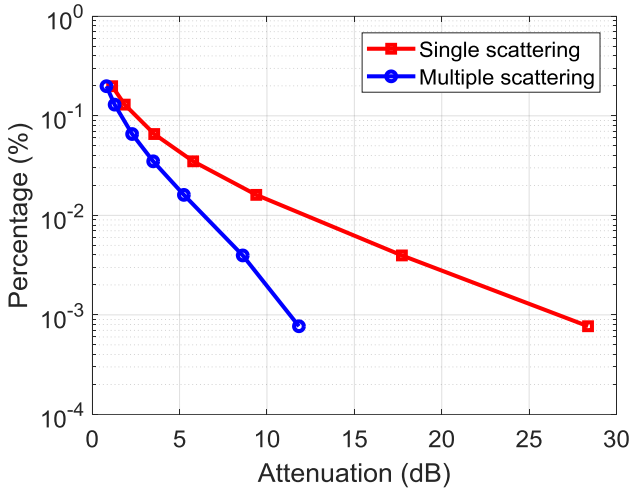

Figure 10. CCDF of rain attenuation over a 1 km path calculated by using the model in Section 2 (single scattering) and by including the effects of multiple scattering. DSD: Gamma type, $\mu = 1$.

5. Conclusions

This manuscript presents a model for the prediction of the attenuation induced by rain on FSO links. The model retains the analytical formulation of the methodology developed by Lin to predict rain attenuation on millimeter-/micro-wave terrestrial links, but employs different rain rate-to-specific attenuation conversion coefficients that were derived for the optical range and for different DSD types using basic single scattering theory. Besides being simple and of quick applicability, the proposed model has been shown to provide accurate predictions, regardless of the path length 1 km $\leq L \leq$ 5 km. The model also takes into account the multiple scattering effects induced by rain, included in terms of a gain that contributes to reducing the overall predicted attenuation. Although additional data are required to corroborate the model's prediction performance, the results obtained in this work are encouraging and suggest that the proposed model represents a useful tool to dimension FSO links in areas where fog is negligible, i.e., where rain is the main impairment to the link performance and availability. Future work includes assessing the prediction accuracy of the proposed model using long-term statistically meaningful experimental data (CCDF of rain attenuation) that are being collected by an FSO link recently installed at Politecnico di Milano for research purposes. Indeed, to the best of the authors' knowledge, no data like these are currently available in the literature to further test the model's prediction accuracy.

Author Contributions: L.L. and R.N. contributed to conceptualization. All the authors contributed to develop the methodology as well as the software tools and to carry out simulations. L.L. and U.A.K. prepared the original draft. All the authors were in charge of writing the revised version of the manuscript. Finally, U.A.K. applied for funding.

Funding: This project was funded by Erasmus Mundus INTACT program, http://www.em-intact.eu/.

Acknowledgments: Umair Ahmed Korai would like to thank the Erasmus Mundus INTACT program, who awarded the staff mobility scholarships (in 2015) for a two-month visit at Politecnico di Milano, Italy.

Conflicts of Interest: The authors declare no conflict of interest.

References

1. Khalighi, M.A.; Uysal, M. Survey on Free Space Optical Communication: A Communication Theory Perspective. *IEEE Commun. Surv. Tutor.* **2014**, *16*, 2231–2258. [CrossRef]
2. Rappaport, T.S.; Sun, S.; Mayzus, R.; Zhao, H.; Azar, Y.; Wang, K.; Wong, G.N.; Schulz, J.K.; Samimi, M.; Gutierrez, F. Millimeter Wave Mobile Communications for 5G Cellular: It Will Work! *IEEE Access* **2013**, *1*, 335–349. [CrossRef]

3. Bloom, S.; Korevaar, E.; Schuster, J.; Willebrand, H. Understanding the Performance of Free-Space Optics. *J. Opt. Commun. Netw.* **2003**, *2*, 178–200.
4. Ijaz, M.; Ghassemlooy, Z.; Perez, J.; Brazda, V.; Fiser, O. Enhancing the Atmospheric Visibility and Fog Attenuation Using a Controlled FSO Channel. *IEEE Photonics Technol. Lett.* **2013**, *25*, 1262–1265. [CrossRef]
5. Andrews, L.C.; Phillips, R.L. *Laser Beam Propagation through Random Media*, 2nd ed.; SPIE: Bellingham, WA, USA, 2005.
6. Clay, M.R.; Lenham, A.P. Transmission of Electromagnetic Radiation in Fogs in the 0.53–10.1 μm Wavelength Range. *Appl. Opt.* **1981**, *20*, 3831–3832. [CrossRef]
7. Chimelis, V. Extinction of CO_2 Laser Radiation by Fog and Rain. *Appl. Opt.* **1982**, *21*, 3367–3372. [CrossRef]
8. Strickland, B.R.; Lavan, M.J.; Woodbridge, E.; Chan, V. Effects of Fog on the Bit-Error Rate of a Free-Space Laser Communication System. *Appl. Opt.* **1999**, *38*, 424–431. [CrossRef] [PubMed]
9. Nebuloni, R.; Capsoni, C. Effect of Adverse Weather on Free-Space Optics. In *Optical Wireless Communications: An Emerging Technology*; Uysal, M., Capsoni, C., Ghassemlooy, Z., Boucouvalas, A., Udvary, E., Eds.; Springer International Publishing: Cham, Switzerland, 2016; pp. 47–68. [CrossRef]
10. ITU-R Recommendation P.530-16. *Propagation Data and Prediction Methods Required for the Design of Terrestrial Line-of-Sight Systems*; ITU: Geneva, Switzerland, 2015.
11. Da Silva Mello, L.A.R.; Pontes, M.S.; Souza, R.M.D.; Garcia, N.A.P. Prediction of Rain Attenuation in Terrestrial Links Using Full Rainfall Rate Distribution. *IEEE Electron. Lett.* **2007**, *43*, 1442–1443. [CrossRef]
12. Lin, S.H. National Long Term Rain Statistics and Empirical Calculation of 11 GHz Microwave Rain Attenuation. *Bell Syst. Tech. J.* **1977**, *56*, 1581–1604. [CrossRef]
13. Moupfouma, F. Electromagnetic Waves Attenuation due to Rain: A Prediction Model for Terrestrial or L.O.S SHF and EHF Radio Communication Links. *J. Infrared Millim. Terahertz Waves* **2009**, *30*, 622–632. [CrossRef]
14. Vasseur, H.; Gibbins, C.J. Prediction of apparent extinction for optical transmission through rain. *Appl. Opt.* **1996**, *35*, 7144–7150. [CrossRef]
15. Carbonneau, T.H.; Wisely, D.R. Opportunities and challenges for optical wireless; the competitive advantage of free space telecommunications links in today's crowded market place. *Proc. SPIE* **1998**, *3232*. [CrossRef]
16. Capsoni, C.; Nebuloni, R. Effect of Rain on Free Space Optics. In Proceedings of the Eleventh URSI Commission F Open Symposium on Radio Wave Propagation and Remote Sensing PUC-RIO, Rio de Janeiro, Brazil, 30 October–2 November 2007; pp. 277–280.
17. Kvicera, V.; Grabner, M.; Fiser, O. Propagation Characteristics Obtained on Parallel Terrestrial FSO Links at 860 nm and 1550 nm. In Proceedings of the 2nd International Workshop on Optical Wireless Communications (IWOW), Newcastle Upon Tyne, UK, 21 October 2013. [CrossRef]
18. Abele, J.; Raidt, H.; Höhn, D.H. Studies on the Influence of Meteorological Parameters on Atmospheric Laser Transmission. *Opt. Acta Int. J. Opt.* **1980**, *27*, 1445–1464. [CrossRef]
19. Luini, L.; Capsoni, C. MultiEXCELL: A New Rain Field Model for Propagation Applications. *IEEE Trans. Antennas Propag.* **2011**, *59*, 4286–4300. [CrossRef]
20. Uppala, S.M.; Kållberg, P.W.; Simmons, A.J.; Andrae, U.; Da Costa Bechtold, V.; Fiorino, M.; Gibson, J.K.; Haseler, J.; Hernandez, A.; Kelly, G.A.; et al. The ERA-40 Re-analysis. *Q. J. R. Meteorol. Soc.* **2005**, *131*, 2961–3012. [CrossRef]
21. Capsoni, C.; Luini, L.; D'Amico, M. The MultiEXCELL Model for the Prediction of the Radio Interference due to Hydrometeor Scattering. In Proceedings of the Forth European Conference on Antennas and Propagation, Barcelona, Spain, 12–16 April 2010; pp. 1–5.
22. Luini, L.; Emiliani, L.; Capsoni, C. Planning of Advanced SatCom Systems Using ACM Techniques: The Impact of Rain Fade. In Proceedings of the Fifth European Conference on Antennas and Propagation, Rome, Italy, 11–15 April 2011; pp. 3965–3969.
23. Luini, L.; Capsoni, C. A Rain Cell Model for the Simulation and Performance Evaluation of Site Diversity Schemes. *IEEE Antennas Wirel. Propag. Lett.* **2013**, *12*, 1327–1330. [CrossRef]
24. Luini, L.; Capsoni, C. A Physically Based Methodology for the Evaluation of the Rain Attenuation on Terrestrial Radio Links. In Proceedings of the Forth European Conference on Antennas and Propagation, Barcelona, Spain, 12–16 April 2010; pp. 1–5.
25. Ghiani, R.; Luini, L.; Fanti, A. A Physically-Based Rain Attenuation Model for Terrestrial Links. *Radio Sci.* **2017**, *52*, 972–980. [CrossRef]

26. Atlas, D.; Srivastava, R.C.; Sekhon, R.S. Doppler Radar Characteristics of Precipitation at Vertical Incidence. *Rev. Geophys. Space Phys.* **1973**, *2*, 1–35. [CrossRef]
27. Ulbrich, C.W. Natural Variations in the Analytical form of the Raindrop Size Distribution. *J. Clim. Appl. Meteor.* **1983**, *22*, 1764–1775. [CrossRef]
28. ITU-R Recommendation P.837-6. *Characteristics of Precipitation for Propagation Modelling*; ITU: Geneva, Switzerland, 2012.
29. Wiscombe, W.J. Improved Mie scattering algorithms. *Appl. Opt.* **1980**, *19*, 1505–1509. [CrossRef]
30. ITU-R Recommendation P.311-15. *Acquisition, Presentation and Analysis of Data in Studies of Tropospheric Propagation*; ITU: Geneva, Switzerland, 2015.
31. Grabner, M.; Kvicera, V. Multiple Scattering in Rain and Fog on Free-Space Optical Links. *J. Lightwave Technol.* **2014**, *32*, 513–520. [CrossRef]